The EMBO Journal (2011) 30, 2246–2254 | © 2011 European Molecular Biology Organization | All Rights Reserved 0261-4189/11
www.embojournal.org

THE EMBO JOURNAL

Conjugal plasmid transfer in *Streptomyces* resembles bacterial chromosome segregation by FtsK/SpoIIIE

Jutta Vogelmann[1], Moritz Ammelburg[2], Constanze Finger[1], Jamil Guezguez[1], Dirk Linke[2], Matthias Flötenmeyer[2], York-Dieter Stierhof[3], Wolfgang Wohlleben[1] and Günther Muth[1,*]

[1]Interfakultaeres Institut für Mikrobiologie und Infektionsmedizin Tuebingen IMIT, Mikrobiologie/Biotechnologie, Eberhard Karls Universitaet Tuebingen, Tuebingen, Germany, [2]Abteilung 1, Proteinevolution, Max-Planck-Institut für Entwicklungsbiologie, Tuebingen, Germany and [3]Zentrum für Molekularbiologie der Pflanzen ZMBP, Eberhard Karls Universitaet Tuebingen, Tuebingen, Germany

Conjugation is a major route of horizontal gene transfer, the driving force in the evolution of bacterial genomes. Antibiotic producing soil bacteria of the genus *Streptomyces* transfer DNA in a unique process involving a single plasmid-encoded protein TraB and a double-stranded DNA molecule. However, the molecular function of TraB in directing DNA transfer from a donor into a recipient cell is unknown. Here, we show that TraB constitutes a novel conjugation system that is clearly distinguished from DNA transfer by a type IV secretion system. We demonstrate that TraB specifically recognizes and binds to repeated 8 bp motifs on the conjugative plasmid. The specific DNA recognition is mediated by helix α3 of the C-terminal winged-helix-turn-helix domain of TraB. We show that TraB assembles to a hexameric ring structure with a central ~3.1 nm channel and forms pores in lipid bilayers. Structure, sequence similarity and DNA binding characteristics of TraB indicate that TraB is derived from an FtsK-like ancestor protein, suggesting that *Streptomyces* adapted the FtsK/SpoIIIE chromosome segregation system to transfer DNA between two distinct *Streptomyces* cells.

The EMBO Journal (2011) **30,** 2246–2254. doi:10.1038/emboj.2011.121; Published online 19 April 2011
Subject Categories: membranes & transport; genome stability & dynamics
Keywords: conjugation; conjugative DNA transfer; FtsK; SpoIIIE; TraB

Introduction

Bacterial conjugation, discovered by Lederberg and Tatum (1946), allows for the transfer of DNA by direct cell-to-cell contact. During conjugative transfer, the DNA molecule has to pass the cell envelopes of a donor and a recipient requiring sophisticated multi-protein translocation machineries composed of about 20 different transfer proteins (Christie *et al*, 2005; Chandran *et al*, 2009). The paradigm of bacterial conjugation, well characterized in Gram-negative and Gram-positive bacteria is the secretion of a pilot protein (relaxase) with a covalently bound single-stranded DNA molecule through the channel of a type IV secretion system (T4SS) (Grohmann *et al*, 2003; Schröder and Lanka, 2003). The transfer is initiated by the plasmid-encoded relaxase, which recognizes a specific sequence, the *oriT*, and induces rolling circle type replication by nicking the plasmid DNA (Willets and Wilkins, 1984). The coupling protein (TrwB/TraG/TraD), a hexameric ring ATPase, interacts with the relaxase that is covalently linked to the 5′ end of the single-stranded plasmid molecule and pumps the protein–DNA complex through the T4SS channel into the recipient (Zechner *et al*, 2000; Christie *et al*, 2005; de la Cruz *et al*, 2010). The relaxase mediates circularization and release of a single-stranded plasmid molecule in the recipient, where it is converted into double-stranded DNA by host factors (Garcillán-Barcia *et al*, 2007; de la Cruz *et al*, 2010).

In *Streptomyces*, filament-forming Gram-positive soil bacteria, which are the producers of ~60% of all known antibiotics, conjugative plasmids are transferred from donors to recipients with high efficiency (Kieser *et al*, 1982; Hopwood and Kieser, 1993). Since antibiotic biosynthetic pathways also include resistance determinants, which were developed to protect the producer from its antibiotic, it was hypothesized that pathogens acquired such resistance genes from the producers by horizontal gene transfer (Davies, 1994; Thomas and Nielsen, 2005; D'Costa *et al*, 2006).

In contrast to plasmid transfer via a T4SS, the unique *Streptomyces* conjugation system involves the transfer of double-stranded DNA (Possoz *et al*, 2001) and requires only a single plasmid-encoded transfer gene *traB* and a small non-coding plasmid region, the *cis*-acting *l*ocus of *t*ransfer *clt* (Pettis and Cohen, 1994; Servín-González, 1996; Grohmann *et al*, 2003). Previously, it was shown that TraB of plasmid pSVH1 (Reuther *et al*, 2006a) binds non-covalently to *clt* of pSVH1 (Reuther *et al*, 2006b). TraB proteins of different *Streptomyces* plasmids form a family of distantly related proteins belonging to the FtsK-like HerA-ATPases, which also include the TrwB/TraG-like coupling proteins (Iyer *et al*, 2004; Gunton *et al*, 2007).

We have analysed purified $TraB_{pSVH1}$ by gel size exclusion chromatography, chemical crosslinking, electron microscopy and single channel conductance measurements and characterized its mode of sequence-specific DNA recognition. We present a previously unknown conjugation mechanism in *Streptomyces*, which is different from all known bacterial gene transfer systems. The similarities in structure and

*Corresponding author. Mikrobiologie/Biotechnologie, Interfakultaeres Institut für Mikrobiologie und Infektionsmedizin Tuebingen IMIT, Eberhard Karls Universitaet Tuebingen, Auf der Morgenstelle 28, Tuebingen 72076, Germany. Tel.: +49 707 129 74637; Fax: +49 707 129 5979; E-mail: gmuth@biotech.uni-tuebingen.de

Received: 1 March 2011; accepted: 25 March 2011; published online: 19 April 2011

function to the chromosomal DNA translocators FtsK and SpoIIIE suggest that antibiotic producing streptomycetes use a segregation-like mechanism, which was originally developed to rescue chromosomal DNA from becoming trapped in the closing division septum for the conjugative DNA transfer between two distinct mycelia.

Results

Streptomyces *TraB proteins closely resemble septal DNA translocators of the FtsK/SpoIIIE family*

Streptomyces TraB proteins are highly diverse, but all show low sequence similarity (<20% identity) to the septal DNA translocators Ftsk/SpoIIIE involved in chromosome segregation and—to an even lower extent—to the coupling proteins involved in plasmid transfer via a T4SS (Gunton *et al*, 2007; Alvarez-Martinez and Christie, 2009). TraB proteins have a domain architecture very similar to that of FtsK (Supplementary Figure S4) with N-terminal transmembrane helices and an ATPase domain containing a nucleotide binding fold with Walker A and B boxes. A phylogenetic tree based on various DNA-translocase domains shows that the similarity of FtsK-like proteins increases from Gram-negative proteobacteria via Gram-positive actinomycetes towards TraB proteins encoded by plasmids of *Streptomyces* and related actinomycetes, suggesting that TraB proteins arose within the *Streptomyces* lineage and diverged rapidly (Figure 1).

The TraB-translocase domain is followed by a C-terminal winged-helix-turn-helix (wHTH) domain involved in sequence-specific DNA binding (Brennan, 1993). The highly divergent wHTH domain of TraB proteins shares significant sequence similarity indicative of homology with the γ-domain of FtsK that also adopts a wHTH fold (Figure 2). The major discriminating feature of TraB to the coupling proteins is the C-terminal wHTH motif, which is absent in all coupling proteins associated with T4SS.

TraB recognizes 8 bp TRS sequences. Streptomyces TraB proteins have a highly specific DNA-binding activity, each one recognizing only its cognate *clt* locus (Franco *et al*, 2003). The TraB-binding site (*clt*) of plasmid pSVH1 contains a series of imperfect GACCCGGA repeats. Since *clt* regions and putative *clt* regions of other *Streptomyces* plasmids also contain 8 bp repeats (Supplementary Figure S1), we speculated that sequence specificity of TraB proteins is determined by recognition of these 8 bp TRS (*T*raB-*r*ecognition *s*equence) motifs. Binding of $TraB_{pSVH1}$ to pSVH1-TRS was studied using oligonucleotides with and without repeated GACCCGGA motifs. In all, 58 nt oligonucleotides corresponding to the + and − strand (referring to the orientation of the upstream *traB* gene) of the *clt* locus were synthesized and labelled with the fluorescence dye Cy5. The + oligonucleotide contained three copies of the 8-bp repeat **GACCCGGA**, while this sequence motif was not present on the complementary − oligonucleotide. In agarose gel retardation experiments,

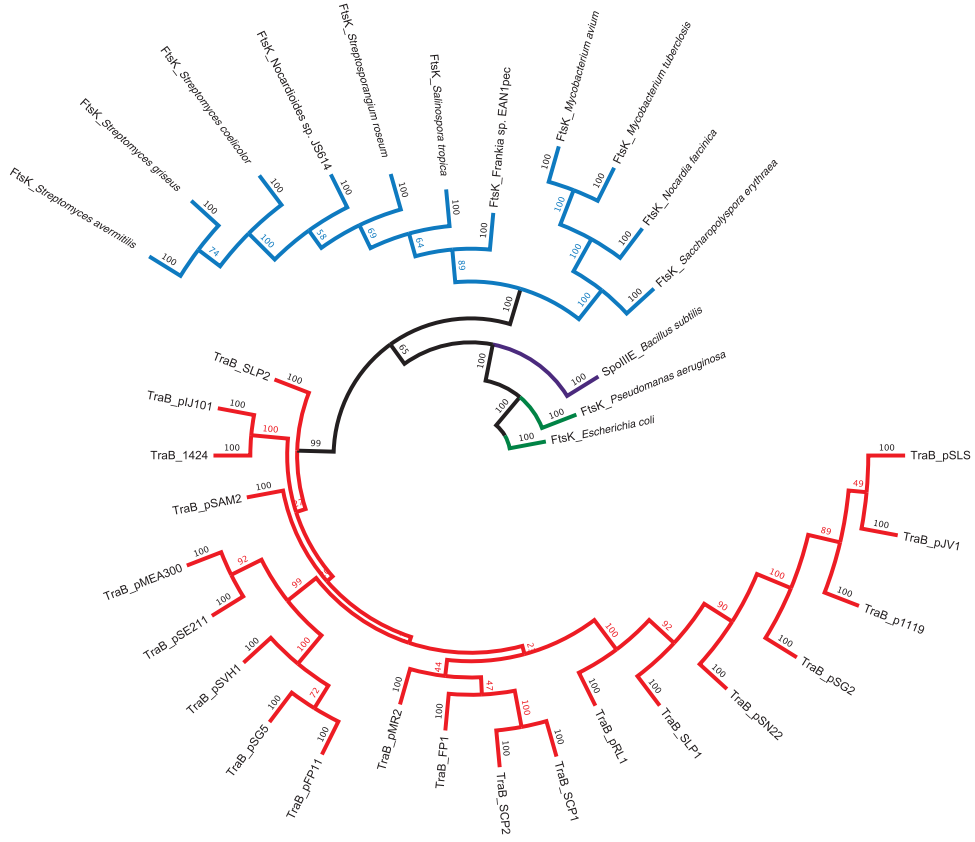

Figure 1 Phylogenic tree of the translocase domain of TraB and FtsK proteins. Multiple sequence alignments of the DNA-translocase domain of selected FtsK and TraB proteins for phylogenetic inference were built using PROMALS 3D (Pei *et al*, 2008). Actinomycetes are displayed in blue, Gram-positive bacteria in magenta and Gram-negative bacteria in green. The tree suggests that the paralogous function of TraB proteins derives from a gene duplication event of *ftsK* or a related gene only in actinomycetes.

A

```
                                α1          α2              α3          β1          β2
TraB group                  hhhhhhhhhhh   hhhhhhhh      hhhhhhhhhhhhhhhh   sss         sss
pSVH1     (689) AAVLEVFAAQATEDDPVDWLPGQLLVDELK---AAGHSVtaek-LGALVVRTDEEKAKRpwgekkt--RVTGypla (758)
pFP11     (679) FNAYDQEAKEENADAAVDWlpGTVLVDALK---AAGLDItpek-LARLVVREDAEKKKRtwedsas--ALNGypla (748)
pSG5      (655) AVVDEFAARSAAAGEELDWlpGAVLLAALK---DTGLDVtaek-LGALVVRTEDEKKANgawegs---RVSGylla (724)
pIJ101    (553) QPTKAPTNREKVAAAIGTGATTVADVAT-----VTGINKgs---VSKAVKQLLDAGEVLrsedgsl--SVVTqvge (618)
p1424     (595) PAAESVSNRDRVFAAVRDGARTNRDVVD-----RTGLNKgt---VSKLVKALVESGELVkdesa----GLLPagga (658)
pSG2      (611) TEEARELLAELVETLAATGGGIVGPADLSPyleQLGRSRpw---VSAELKRLAAEGRLAptaeegry-RVLPvpva (682)
SLP1      (609) PEEARELFAAALAEFEQSGQMIVGPKDFTDwcdRHNLGRsw---VSKRLKEAAEEGRLQatnttgrw-RIVPamaa (680)
pJV1      (606) PEEARELLEDMVAMLAGVGPGTVAVKDLGPyleQLGRDRsw---VSKQMSRMASEGRLAptaeqgvy-RLVPvlaa (677)
p1119     (601) PEEARELLDEMVRMLASVGSGTVSVRDVTPyldRIGRDRsw---VSKEMKKLAEEGRLAptgeqgvy-RLIAtmaa (672)
pSN22     (579) TEEARELLDEMVATLASVGPGTVAVRDLKPyleQIGRDRsw---VSREMKRMAEEGRLAatgeegvy-RLIPtlag (650)
pSLS      (600) PEEARELLDELVRMLAGMGPGTVAVKDLGPyleQLGRDRsw---VSKEMKRLAEEGLVPv---lagv--------- (660)
pMEA300   (686) APQVRDLLDDVAEVIAGADVKATDVGARLRkl-APGYEPyanltAEKVKEALEAVGVPVrlkqgiitvRARHvana (760)

FtsK group
Sc-FtsK   (849) IGDDLDLLCQAAELVVSTQFGSTSMLQRKL---RVGFAK-----AGRLMDLMESRSIVGPSEGSKA--RDVLvkpd (915)
Bs-FtsK   (715) SEVTDELYDEAVELIVGMQTASVSMLQRRF---RIGYTR-----AARLIDAMEERGVVGPYEGSKP--REVLlske (780)
Pa-FtsK   (743) GSEDDPLYDEAVRFVTESRRASISAVQRKL---KIGYNR-----AARMIEAMEMAGVVTpmntngs--REVIapap (808)
Ec-FtsK  (1262) AEELDPLFDQAVQFVTEKRKASISGVQRQF---RIGYNR-----AARIIEQMEAQGIVSeqghngn--REVLappp(1327)
Mt-FtsK   (803) IGDDMDVFLQAVELVVSSQFGSTSMLQRKL---RVGFAK-----AGRLMDLMETRGIVGpsegska--REVLvkpd (869)
PFAM        (1) SEEEDELYEEAVELVVETQKASTSLLQRRL---RIGYNR-----AARIIDQLEEEGIVSpangskp--REVLvtke  (66)
```

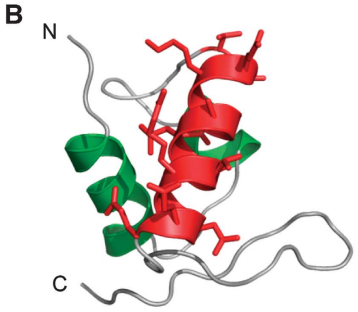

Figure 2 The C-terminal winged-helix-turn-helix domain (wHTH) of selected DNA-translocator proteins. (**A**) Alignment of the wHTH motifs of selected TraB and FtsK proteins. Helices α1 and α2 are given in green letters, helix α3 in red letters. Blue letters indicate strand β1 and strand β2, which form the wings. A consensus of the predicted secondary structure is shown above the sequences (h, helix; s, strand). Letters in lower case denote residues of unsure equivalence. Sequences are ordered by similarity according to which wHTH domains of TraB and FtsK constitute the major groups. The order generally matches the pattern observed in the phylogenetic tree (Figure 1). The alignment shows pronounced differences in helix α3, which has a crucial role in specific DNA binding. This may reflect the affinity of a particular wHTH domain to the corresponding 8 bp repeats found in its cognate plasmid (Supplementary Figure S1). (**B**) Model of the $TraB_{pSVH1}$ wHTH domain generated by Modeller (Sali and Blundell, 1993) using the γ-domain of *P. aeruginosa* FtsK as a template. Helices α1 and α2 are given in green, while helix α3, proposed to determine sequence-specific DNA recognition is drawn in red colour.

TraB shifted only the oligonucleotide containing the 8 bp sequence motifs, but did not bind to the complementary oligonucleotide lacking this sequence motif (Figure 3A).

Also, synthetic double-stranded 24 bp oligonucleotides, TRS_0 and TRS_2 (containing two copies of the GACCCGGA sequence), were generated by annealing complementary oligonucleotides and incubated with $TraB_s$ and TraB. Only oligonucleotide TRS_2 containing two copies of the TRS GACCCGGA was retarded, TRS_0 lacking the repeats was not shifted (Figure 3B). TRS were recognized by TraB and $TraB_s$, a soluble derivative that lacks the N-terminal 270 membrane-associated amino acids, revealing that the N-terminus of TraB is not involved in specific DNA recognition.

Binding of TraB to 8 bp TRS resembles the reported interaction of *Escherichia coli* FtsK with 8 bp KOPS (Fts*K* *O*rienting *P*olar *S*equences) (Bigot *et al*, 2005; Löwe *et al*, 2008). Whereas KOPS are distributed over the whole chromosome with a strong bias from the origin towards the terminus region, repeated TRS on a given plasmid are exclusively found in the *clt* region (Supplementary Figure S1).

Whereas transfer of chromosomal genes by the T4SS requires integration of the plasmid into the chromosome, conjugative transfer of chromosomal genes in *Streptomyces* conjugation can occur without plasmid integration (Pettis and Cohen, 1994). An explanation is provided by the identification of TraB-binding sites in the *Streptomyces coelicolor* chromosome. Using PatScan (Dsouza *et al*, 1997) analysis, the clt_{pSVH1}-like motif GACCCGGA-N_{0-13}-GACCCGGA-N_{0-13}-GACCCGGA-N_{0-13}-GACCCGGA (allowing one mismatch per motif) was identified 25 times (Supplementary Figure S2). These regions were statistically distributed and localized in 21 of 25 cases to coding regions. We analysed two of the predicted *clt-l*ike *c*hromosomal sequences (*clc*) by gel retardation assays with purified $TraB_s$ (Figure 4). Both *clc* sequences were efficiently bound by $TraB_s$. In the *clc* sequences identified by PatScan only the 8-bp TRS repeats are conserved, whereas their distance and the intervening sequences are highly variable. This supports the finding that only the 8 bp TRS repeats are critical for TraB binding.

Helix α3 of the TraB wHTH motif determines sequence-specific DNA recognition. Despite their sequence divergence (Figure 1), all TraB proteins have the same domain organization with N-terminal transmembrane helices and an ATPase domain followed by a C-terminal wHTH domain (Supplementary Figure S3). To identify the TraB region involved in sequence-specific TRS recognition, we constructed chimeric TraB proteins by fusing parts of *traB* genes from different *Streptomyces* plasmids (Supplementary Tables S5 and S6; Supplementary Figure S4A).

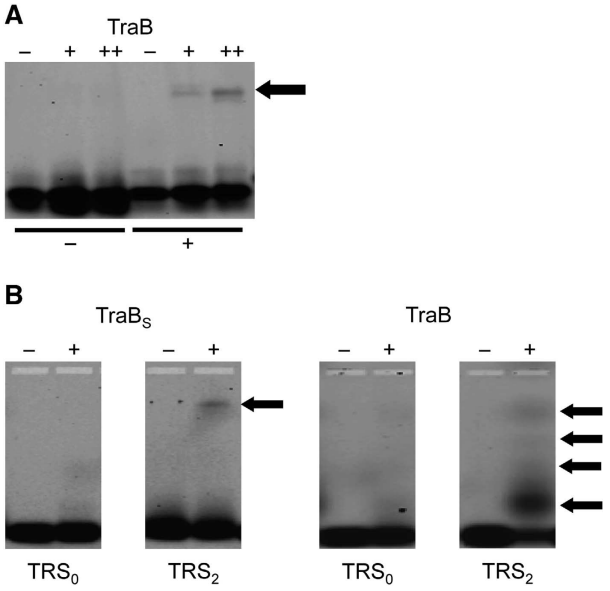

Figure 3 Gel retardation assays demonstrating specific interaction of TraB with TraB-recognition sequences (TRS). (**A**) Gel shift with 58 nt oligonucleotides comprising the minimal TraB-binding site. clt$^+$ oligonucleotide, containing two perfect and one imperfect TRS repeats or the complementary strand (clt$^-$, lacking any TRS repeat) were Cy5 labelled and analysed for TraB (−: 0 μg, +: 1.5 μg, ++: 3 μg) binding. Visualization of the bands by fluorescence laser scanning revealed that TraB shifted only the clt$^+$ strand (arrow) containing the TRS repeats. (**B**) Gel shift assay with synthetic double-stranded oligonucleotides. In all, 24 bp oligonucleotides TRS$_0$ and TRS$_2$ (containing two copies of the GACCCGGA sequence) were incubated with TraB$_s$ (left) and TraB (right). TraB and TraB$_s$ bind (arrow) only to TRS$_2$, while TRS$_0$ was not bound. The multiple retarded bands observed upon binding of full-length TraB probably reflect different oligomerization states of TraB. −: no protein added; +: 8 μg TraB$_s$ or 0.5 μg TraB.

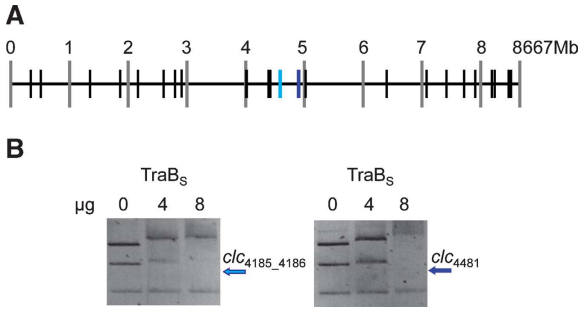

Figure 4 TraB$_s$ also binds to *clt*-like chromosomal (*clc*) sequences. (**A**) Distribution of the *clc*$_{pSVH1}$ sequences on the linear chromosomal map of *S. coelicolor*. The *clc* sequences that were confirmed for TraB binding by gel retardation assays are highlighted in blue. (**B**) Gel retardation assay with subcloned *clc* sequences. *S. coelicolor clc* sequences present within SCO4481 and in the intergenic region between SCO4185 and SCO4186 were amplified, subcloned into a cloning vector and digested to yield three DNA fragments. The intermediate sized fragment contained the cloned *clc* sequence. Gel retardation assays with different amounts of TraB$_s$ (0, 4, 8 μg) demonstrated that only the *clc* containing DNA fragment is retarded (arrows), while the other fragments that serve as negative controls are not shifted.

The chimeric fusion proteins that included all TraB domains were expressed in *E. coli* with an N-terminal strep-tagII sequence and purified by affinity chromatography.

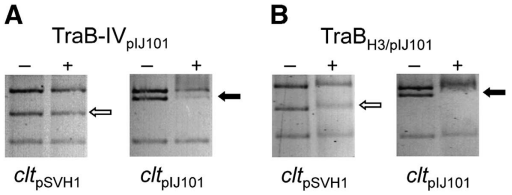

Figure 5 Helix α3 of the TraB wHTH motif determines sequence-specific DNA recognition. (**A**) Gel retardation experiment with chimeric TraB-IV$_{pIJ101}$ protein. *clt* sequences of plasmids pSVH1 and pIJ101 were subcloned into a cloning vector, digested to yield three DNA fragments and used in gel retardation assays with chimeric TraB proteins. The *clt* containing DNA fragment is indicated with an arrow. TraB-IV$_{pIJ101}$, containing the N-terminal 702 aa of TraB$_{pSVH1}$ and the 70 aa C-terminal wHTH domain of TraB$_{pIJ101}$ has lost its ability to interact with *clt*$_{pSVH1}$ (open arrow) but binds *clt*$_{pIJ101}$ (black arrow). (**B**) Exchange of helix α3 of TraB$_{pSVH1}$ against α3 of TraB$_{pIJ101}$ is sufficient to switch *clt* recognition. TraB$_{H3pIJ101}$ binds to the *clt* of plasmid pIJ101, while *clt*$_{pSVH1}$ is not recognized. −no protein; +: 0.1–0.3 μg protein.

The purified proteins were analysed by gel retardation assays for their interaction with different *clt*-loci (Figure 5A; Supplementary Figure S4B–I).

Replacing the C-terminal 343 aa of TraB$_{pSVH1}$ by the 344 C-terminal aa of TraB$_{pIJ101}$ generated a chimeric protein (TraB-II$_{pIJ101}$) that did not bind to the *clt* of plasmid pSVH1 but shifted the *clt* of plasmid pIJ101 (Supplementary Figure S4D and E). Localization of the DNA-binding region to the C-terminal TraB half was confirmed by fusing the C-terminal 344 aa of TraB$_{pIJ101}$ to the maltose-binding protein (MBP-II$_{pIJ101}$; Supplementary Table S6). This fusion protein specifically recognized the *clt* locus of plasmid pIJ101 (Supplementary Figure S4C). Also, TraB-III$_{pIJ101}$ carrying the N-terminal 566 aa of TraB$_{pSVH1}$ and the very last 157 aa of TraB$_{pIJ101}$ only bound to the *clt* of plasmid pIJ101 (Supplementary Figure S4F and G).

To further narrow down the DNA-binding region, the very last 70 aa of TraB$_{pSVH1}$ encoding the wHTH domain, were replaced by the corresponding parts of TraB$_{pIJ101}$ and TraB$_{p1119}$, respectively (Supplementary Table S6). Exchange of only the wHTH domain changed *clt* recognition (Figure 5A; Supplementary Figure S4H and I), demonstrating that the wHTH motif at the TraB C-terminus determines sequence-specific DNA binding for each TraB-*clt* pair.

Since the structures of wHTH domains (Figure 2B) suggest that in particular helix α3 is crucial for DNA recognition (Löwe *et al*, 2008), we constructed a chimeric TraB protein in which only helix α3 was exchanged. Helix α3 (SVTAEKLGALVVRTD) of TraB$_{pSVH1}$ was replaced by helix α3 (NKGSVSKAVKQLL) of TraB$_{pIJ101}$, generating a protein (TraB$_{H3pIJ101}$) that specifically recognized *clt* of pIJ101 but had lost its ability to interact with *clt*$_{pSVH1}$ (Figure 5B). This proves the important role of helix H3 in determining DNA recognition for proteins of the FtsK-HerA family.

Structure of TraB. As conjugative DNA transfer involves DNA translocation across cell envelopes of donor and recipient, a DNA translocation channel spanning membranes and peptidoglycan (PG) layers has to be postulated. In PG-binding assays with purified PG of *S. coelicolor*, we demonstrated the ability of TraB to interact with PG (Supplementary Figure S5A and B). Chemical crosslinking of TraB$_s$ showed high molecular

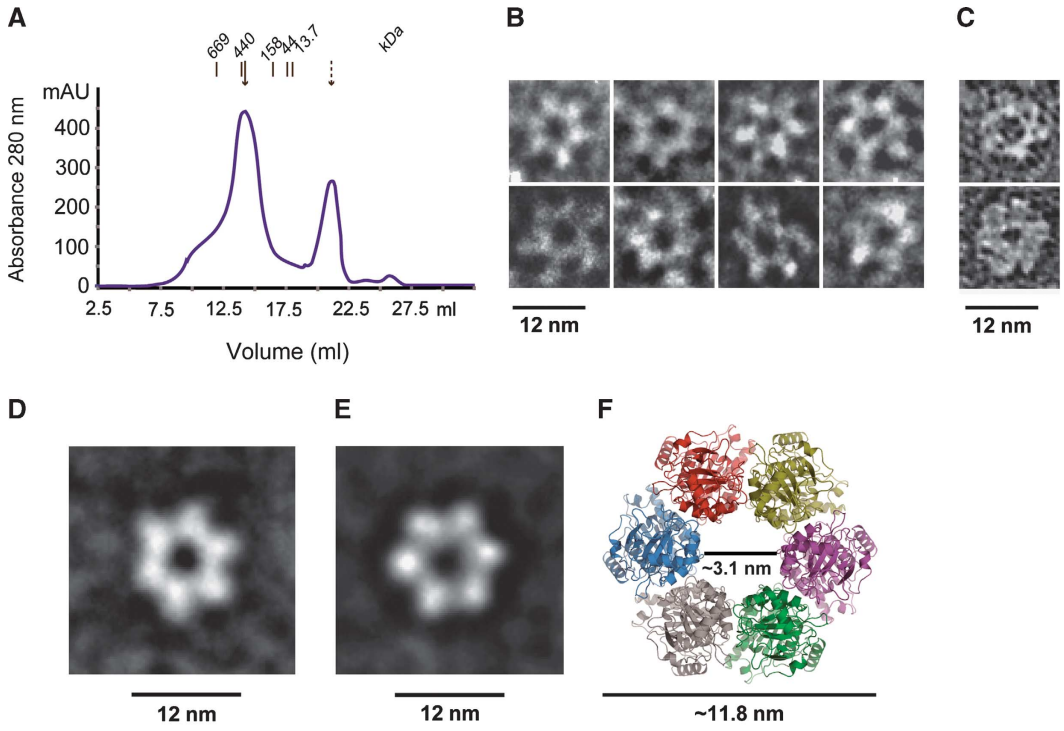

Figure 6 Electron microscopy of $TraB_{pSVH1}$ shows hexameric ring-shaped structures with a central pore. (**A**) Elution profile of $TraB_s$ on a Superose 6 column demonstrating oligomerization of $TraB_s$. Black lines indicate molecular weight standards. Under the assayed conditions (10 mM $MgCl_2$, 2 μM ATPγS), $TraB_s$ mainly eluted as a high molecular weight oligomer (black arrow). Free ATPγS eluted at 21.3 ml (dashed arrow). (**B**, **C**) Negative stain electron micrographs of TraB. Manually selected $TraB_s$-hexamers (**B**) and full-length TraB-hexamers (**C**) greatly resemble each other in size and six-fold symmetry. (**D**, **E**) 2D averaging of electron microscopic images. Representative classes of averaged $TraB_s$-hexamers (**D** ($n = 33$), **E** ($n = 90$)) show a diameter of ~12 nm and a pore size of about 3.1 nm (**D**) −3.5 nm (**E**). (**F**) Homology modelling of the TraB DNA-translocase domain. The $TraB_{pSVH1}$-translocase domain was modelled based on the *P. aeruginosa* FtsK DNA-translocase domain. The modelled TraB structure shows a six-fold symmetry with a diameter of ~11.8 and an ~3.1 nm pore, sufficient for translocation of a double-stranded DNA molecule.

weight TraB complexes, and thus oligomerization (Supplementary Figure S6). In bacterial two-hybrid analyses (Karimova *et al*, 1998), we obtained evidence that both the N-terminal 130 aa and the C-terminal wHTH domain of TraB are involved in oligomerization (Supplementary Figure S7). Analytical gel filtration of $TraB_s$ suggested a hexameric conformation (Figure 6A). Using electron microscopy we detected ring-shaped hexameric structures of TraB resembling those of the DNA-translocase domain of *Pseudomonas aeruginosa* FtsK (Massey *et al*, 2006). Interestingly, soluble $TraB_s$ lacking the N-terminal 270 aa membrane-anchor region (Figure 6B) produced similar hexameric complexes as full-length TraB (Figure 6C). In all, 1214 manually selected $TraB_s$ images were processed by 2D averaging using EMAN2 (Ludtke *et al*, 1999; Tang *et al*, 2007) software suite (Figure 6D and E; Supplementary Figure S8). Representative classes of averaged $TraB_s$-hexamers show a diameter of ~12 nm and a pore size of about 3.1 nm (Figure 6D ($n = 33$)) and 3.5 nm (Figure 6E ($n = 90$)), respectively. Using the related structure of the *P. aeruginosa* FtsK DNA-translocase domain, we modelled the corresponding TraB region with Modeller (Sali and Blundell, 1993). Based on high quality sequence alignments, a feasible TraB-model showing a six-fold symmetry with a central pore size of 3.1 nm was built (Figure 6F), which is in good agreement with the electron microscopic images. In contrast to the hexameric ring ATPase TrwB, which has a central channel of ~2 nm (Gomis-Rüth *et al*, 2001) and translocates single-stranded DNA, the TraB channel has a channel of about 3.1 nm and thus is big enough to translocate double-stranded DNA.

TraB forms pores in lipid bilayers in vitro

For proteins of the FtsK/SpoIIIE family it is a matter of debate whether the translocation process involves the formation of a membrane pore or not. Whereas SpoIIIE was reported to transport DNA across fused septal membranes during sporulation in *Bacillus subtilis* (Burton *et al*, 2007), FtsK of *E. coli* does not necessarily have to transcend membranes in the closing septum and pore formation may not be required (Dubarry and Barre, 2009).

Since conjugative DNA transfer between two distinct cells is highly unlikely without pore formation, we performed TraB single channel conductance measurements using planar lipid bilayers. After adding TraB (0.05–0.5 μg) to the *cis*-side of the membrane, TraB inserted spontaneously into the membrane at various voltages (Figure 7A; Supplementary Figure S10A and B), revealing two distinct conductance states c1 and c2 (Supplementary Figure S10A–C). The observed current steps were consistently obtained with different samples of purified TraB protein (Figure 7A).

Since in planar bilayer experiments single channels are measured, they are notorious for giving false-positive signals. To exclude contamination with outer membrane porins, the most frequent pore-forming contaminant, TraB was isolated from *Streptomyces lividans* and purified to single band purity as visualized by silver staining (Supplementary Figure S9).

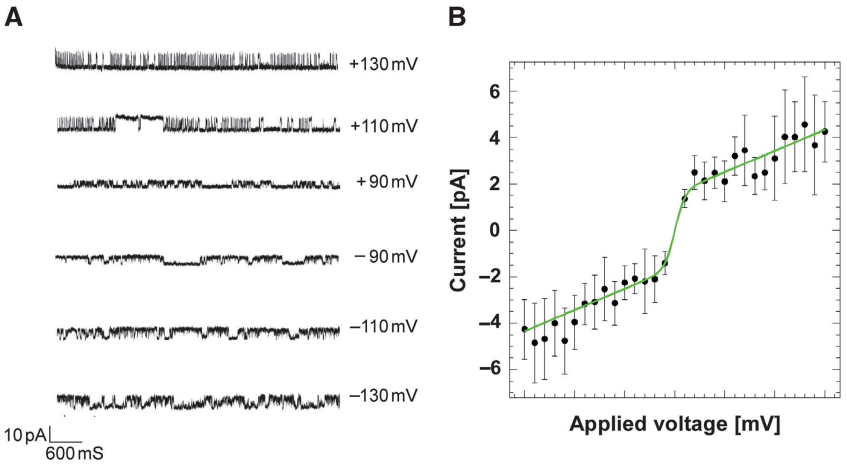

Figure 7 $TraB_{pSVH1}$ forms pores in lipid bilayers *in vitro*. (**A**) Single channel recordings of $TraB_{pSVH1}$ pores. Representative traces (conductance level c1) of TraB single channel recordings at different voltages are given. The distribution of c1 conductance is shown in Supplementary Figure S10. (**B**) Current–voltage relationship of TraB channels. Symmetric but mostly non-linear behaviour of the measured current is observed in 200 mM NaCl (sigmoidal fit in green).

To further prove that the channel recordings (Figure 7; Supplementary Figure S10) were caused by TraB and not by co-purified contaminating proteins, the following control experiments were carefully performed. First, a *S. lividans* culture carrying the empty expression vector pGM190 was identically processed as the TraB expressing strain. Elution fractions of this purification (no protein bands detected by silver staining) did not cause pore signals in single channel recordings. To rule out any contaminating protein interacting with TraB itself, $TraB_s$ (Supplementary Table S6), which lacks the transmembrane region was expressed in *S. lividans* and purified under identical conditions (Supplementary Figure S9C). As an additional control, N-terminal strepII-tagged GlnE, a 110-kDa adenylyltransferase involved in nitrogen metabolism of *S. coelicolor* (M Nentwich, personal communication) was purified from *S. lividans* (Supplementary Figure S9D), applying the same protocol as for TraB. Using these controls, each of the channel recordings was done in a range between ±10 and ±150 mV and repeated 2–3 times. Each applied voltage step was carried out for about a minute. In contrast to TraB, neither the addition of the soluble $TraB_s$, protein that lacks the membrane-anchor region, nor the addition of the other negative controls resulted in any channel occurrence in the experimental setup for a measured time period of about 30 min.

For TraB measurements between 10 and 90 mV, the dominating conductance state that was observed frequently for most channels (73.9%) was c1, whereas only 26.1% of the observed pores showed conductance state c2. The application of voltages of ±100 and ±150 mV resulted in only one state of lower conductance (c1). The observed TraB-pores show a voltage dependence of the conductance state c1 that is symmetric, but does not show a clear ohmic behaviour in 200 mM NaCl; at voltages above +30 mV and below −30 mV, saturation is observed (Figure 7B). Interestingly, significant differences concerning the open time behaviour of c1 pores (110–150 mV) were observed between positive and negative voltages. Averaged open time for positive voltages (+110 to 150 mV) was 47–81 ms while for negative voltages (−110 to 150 mV) an open time of 105–200 ms was recorded. At positive voltages, only 14.2% of the pores opened longer than 100 ms, whereas at negative voltages 38.6% had an open time exceeding 100 ms (Supplementary Figure S11). This difference might reflect the *in vivo* situation with a negative membrane potential (Miller and Koshland, 1977) that in the given experimental setup corresponds to a positive-applied voltage. Details on the pore characteristics are given in Supplementary Figures S10 and S11. Neither the addition of ATP/ATPγS (1 mM) nor the addition of circular plasmid DNA affected channel formation, conductance or open times (data not shown). This is in line with the analyses of ATPase activities of $TraB_{pSVH1}$, which were also not influenced by the addition of plasmid DNA (Reuther *et al*, 2006b).

We demonstrate here for the first time that a DNA translocator of the FtsK/SpoIIIE family forms pores in artificial membranes.

Discussion

All plasmid-encoded conjugation systems characterized so far translocate the DNA through a T4SS (Zechner *et al*, 2000; Grohmann *et al*, 2003; Christie *et al*, 2005). The key components of bacterial T4SS conjugation machinery are the relaxases and the TrwB-like coupling proteins, hexameric ring ATPases that transfer the relaxase as a pilot protein with a covalently linked plasmid molecule into the recipient cell (Gomis-Rüth *et al*, 2001; Schröder and Lanka, 2003). Although *Streptomyces* TraB proteins show similarity to the coupling proteins (Alvarez-Martinez and Christie, 2009), they are clearly distinguished from this class of transfer proteins and they promote gene transfer by a completely different mechanism. Coupling proteins lack a wHTH domain and do not have a specific DNA-binding activity. They recognize the single-stranded DNA-bound relaxase (Schröder and Lanka, 2003; Christie *et al*, 2005; de la Cruz *et al*, 2010) and transfer this protein–DNA complex through a central 2 nm channel (Gomis-Rüth *et al*, 2001). In contrast, TraB has a highly specific DNA-binding activity recognizing 8 bp TRS repeats within the *clt* region of a given plasmid. In most plasmids, the *clt* is located next to the *traB* gene and contains distinct 8 bp

TRS repeats. *Streptomyces* conjugation does not involve a specific relaxase and TraB has to translocate a double-stranded DNA molecule through an ~3.1 nm channel.

The existence of *clt*-like sequences on the chromosome of *S. coelicolor*, which are also bound by TraB specifically, discloses a new mechanism of chromosome mobilization distinct from HFR (*h*igh *f*requency of *r*ecombination)-mating in the T4SS conjugation system. Whereas in HFR-matings, the mobilization of chromosomal DNA is dependent on the preceding integration of the plasmid (and its *oriT*) into the chromosome (Thomas and Nielsen, 2005), transfer of chromosomal DNA during *Streptomyces* conjugation does not require an integrated plasmid (Pettis and Cohen, 1994). Demonstration that TraB does not exclusively recognize the *clt* locus of plasmid pSVH1 for plasmid transfer, but also interacts with chromosomal *clc* sequences (Figure 4), clearly suggests that mobilization of chromosomal DNA in *Streptomyces* does not depend on a physical interaction of the plasmid with the chromosome.

To experimentally localize the TraB region determining sequence-specific DNA recognition, four different TraB proteins ($TraB_{pSVH1}$, $TraB_{pSG5}$, $TraB_{pIJ101}$ and $TraB_{p1119}$), selected with regard to their degree of similarity (Figure 1), were used for the construction of chimeric proteins. Using these proteins, specific DNA recognition could be analysed by comparing efficiency of DNA binding to two different *clt* loci. Only proteins, able to recognize a specific *clt* locus were used to narrow down the *clt*-interacting region. The gel retardation experiments localized the *clt*-recognition domain to the very C-terminus of TraB. This confirmed bioinformatic analyses, which predict a wHTH fold to this region.

TraB resembles the septal chromosome-translocator protein FtsK/SpoIIIE in sequence, domain organization and hexameric structure, indicating that TraB is derived from an FtsK-like ancestor protein. Furthermore, the mode of TraB binding to *clt* via recognition of 8 bp TRS is reminiscent of the interaction of FtsK with 8 bp KOPS (Löwe *et al*, 2008). This suggests that TraB translocates plasmid DNA using a molecular mechanism similar to the FtsK/SpoIIIE chromosome segregation system. Even though proteins of the TraB/FtsK/SpoIIIE family are highly similar in many aspects, their cellular function differs substantially. The FtsK system finds and positions chromosomal *dif* sites for dimer resolution and moves chromosomal DNA away from the closing septum (Massey *et al*, 2006; Burton *et al*, 2007; Ptacin *et al*, 2008). During chromosome segregation, the DNA is already present in the closing septum. The membrane-associated FtsK/SpoIIIE can easily assemble around a chromosomal arm and translocate the chromosomal DNA without the need of a translocation pore in the septum (Dubarry and Barre, 2009).

In contrast, TraB has to translocate circular plasmid DNA from the donor into the recipient. Whereas FtsK is a septal DNA translocator and localizes to the division septum (Yu *et al*, 1998), $TraB_{pSG5}$ was detected at the mycelial tips (Reuther *et al*, 2006b). The pore-forming ability of TraB suggests that TraB forms a channel at the hyphal tips to promote DNA translocation to the recipient. How to pump an unbroken circular DNA molecule through the cell envelopes of donor and recipient remains unclear. Since TraB is apparently the only plasmid-encoded protein involved in this process (Pettis and Cohen, 1994), TraB must either recruit other cellular enzymes or possess further enzymatic activities waiting to be elucidated.

Materials and methods

Bacterial strains and media

Cultivation of strains and procedures for DNA manipulation were performed as previously described for *E. coli* (Sambrook and Russel, 2001) and *S. coelicolor* (Kieser *et al*, 2000). Proteins were purified from *E. coli* BL21 (DE3)-pLys (Invitrogen) and *S. lividans* strains TK64 and TK23 (Kieser *et al*, 2000). Plasmids are listed in Supplementary Table S1. Oligonucleotides used for DNA-binding studies are given in Supplementary Tables S3 and S4, respectively.

Heterologous expression and purification of strepII-TraB proteins

TraB fragments were amplified from templates pJR201, pIJ101, p1119 and pEB211 (Supplementary Table S1), respectively, using primers listed in Supplementary Table S2. Some of the chimeric constructs were fused via restriction sites, others via overlap extension PCR (Higuchi *et al*, 1988) (Supplementary Tables S5 and S6). For protein expression in *E. coli*, an overnight culture (LB, 37°C) was induced with rhamnose at a final concentration of 0.2% for 6 h at 30°C. For expression in *S. lividans*, cells were grown in S-medium (50 μg/ml kanamycin, 72 h), induced with thiostrepton (10 μg/ml) and incubated at 27°C for additional 12 h. Cells were harvested by centrifugation, resuspended in lysis buffer (50 mM Tris, pH 8.0, 1 M NaCl, 2% Triton X-100, protease inhibitor mix (Roche), 5 μg/ml DNaseI and 10 mM mercaptoethanol). Cells were broken by French pressing and soluble proteins were separated by centrifugation at 21 000 *g* for 10 min.

StrepII-TraB and strepII-GlnE fusion proteins were purified at 4°C using StrepTactin-Sepharose (IBA, Göttingen, Germany) according to the manufacturer's instructions. $TraB_s$ affinity purification was followed by preparative gel filtration on a Superdex S200 column in 20 mM Hepes, pH 7.2, 150 mM NaCl, 1 mM DTT. Fractions containing $TraB_s$ were concentrated to a final concentration of 7 mg/ml

Gel-sizing chromatography

Analytical gel-sizing chromatography was performed with 0.25 ml of protein solution at 8°C on a Superose 6 column equilibrated with 20 mM Hepes, pH 7.2, 150 mM NaCl, 1 mM DTT, 10 mM $MgCl_2$ and 2 mM ATPγS. Before injection, $TraB_s$ was incubated in the presence of 2 mM ATPγS and 10 mM $MgCl_2$ for 1 h at room temperature. The apparent molecular mass was determined from the elution volume, using a calibration curve obtained with suitable standard proteins (thyroglobulin ($M_r = 669.000$), ferritin ($M_r = 440.000$), aldolase ($M_r = 158.000$), ovalbumin ($M_r = 44.000$) and RNase ($M_r = 13.700$); Figure 6A).

Agarose gel mobility shift assay

Approximately 0.5 μg digested plasmid DNA (pCG-clt, pD-clt101, pD-clt1119, pD-clcI, pD-clcII: ApaLI/*Pst*I; pIJ101 *Nco*I/*Spe*I) or 0.3–0.57 ng of Cy5-labelled oligonucleotides were incubated with different amounts (0–36 pmol, depending on the construct) of purified TraB protein in 50 mM Tris/HCl pH 7.0–9.0, 200 mM NaCl, 10 mM $MgCl_2$). DNA-binding reactions were performed on ice for 2–10 min, gel loading solution (50% glycerol, 50 mM Tris/HCl pH 8.0) was added and the reaction mixture was separated on either a 1–2% TAE agarose gel or analysed by a native 8% PA gel (Tris-Glycin). DNA was stained with ethidiumbromide or visualized using a Typhoon (GE Healthcare) fluorescence laser scanner (for Cy5-labelled oligonucleotides).

Glutaraldehyde crosslinking

About 5 μg purified TraB protein was crosslinked in a final volume of 30 μl 20 mM Tris/pH 7.6, 130 mM NaCl, 6 mM $MgCl_2$ by the addition of glutaraldehyde to a final concentration of 0.03%. After incubation for 1 h on ice, the reaction was stopped by adding 1 M glycin to a final concentration of 100 mM. After boiling, samples were analysed by 4–12% Tris-Tricin SDS PA gel (ClearPAGE™, C.B.S. Scientific).

PG-binding assay

PG was isolated from *S. lividans* according to Ursinus *et al* (2004). Proteins (1–10 μg) were mixed with 100 μg PG in a total volume of 100 μl 0.1 N NaAc pH 5.4 and incubated (room temperature, 30 min). Samples were centrifuged (30 min at 4°C, 21 000 *g*) and the supernatant containing the unbound proteins was collected. Bound proteins remaining in the pellet were dissolved in 100 μl 2% SDS and incubated under shaking for 1 h at 37°C. Samples were again centrifuged (21 000 *g*, 30 min at 4°C) and the supernatants were analysed by SDS–PAGE. Ami-$R_{1,2}$ used as a positive control was a kind gift of M Schlag, Tübingen.

Immunoblot analysis

For immunological detection, TraB and its derivatives were separated on a 12.5% SDS PA gel and transferred to a nitrocellulose membrane by electroblotting (The W.E.P. Company). Membranes were blocked for 1 h (5% milk powder in TBST), washed and incubated with rabbit-anti-TraB-IgG serum for 1 h followed by several washing steps (1% milk powder in TBST). Following incubation with peroxidase-conjugated anti-rabbit-IgG, the blot was developed using a Western Lightning® Plus-ECL (Perkin-Elmer) solution and analysed on a Molecular Imager® *ChemiDoc*™ *XRS* System (Bio-Rad).

Electron microscopy and image processing

For negative staining, hexameric $TraB_s$ was incubated in buffer A (20 mM Hepes, pH 7.2, 150 mM NaCl, 1 mM DTT, 10 mM $MgCl_2$, 2 mM ATPγS) for 20 min at room temperature and diluted to a final protein concentration of 0.01–0.5 μg/μl. Aliquots were applied to glow-discharged carbon-coated EM-grids, washed with distilled water and stained with 1% aqueous uranyl acetate. Samples were examined in a LEO 906 transmission electron microscope at an accelerating voltage of 80 kV ($TraB_{pSVH1}$) or a Tecnai T12 Spirit BioTwin transmission electron microscope (FEI, Endhoven, The Netherlands) at an accelerating voltage of 120 kV ($TraB_s$). Images were recorded at ×30 000 (overview) – ×49 000 magnification with a USC 4000 CCD camera (Gatan, Pleasanton, CA), 2 μm under-focus, 4000 × 4000 pixel. The pixel size of the digital images at ×49 000 magnification was 2.311 Å/pixel.

The EMAN2 software suite (Ludtke *et al*, 1999; Tang *et al*, 2007) was used to perform 2D averaging of $TraB_s$. In brief, raw images (×49 000 magnification) were imported and edge normalized. In total, 1214 $TraB_S$-hexamer particles were selected manually from the digitized electron micrographs using EMAN's *boxer* and boxed with a box size of 160 × 160 pixels. Following the EMAN2 workflow, the particle images were subjected to a CTF-correction, then rotationally and translationally aligned, classified in 19 classes (classkeep = 0.8) and finally class averages were calculated (Supplementary Figure S8).

Electrophysiology

Single channel conductance values were recorded at room temperature using a BLM workstation (Warner Instruments, Hamden, CT), with a pair of chlorinated silver electrodes, a BC-535 amplifier and an LPF-8 Bessel filter connected to an Axon Digidata 1440A digitizer. Data were recorded and evaluated using pCLAMP 10.0 software (Molecular Devices, Sunnyvale, CA). A commercial polysulfone cuvette (Warner Instruments) with two compartments (1.5 ml each) connected by a 150-μM aperture was used. Black lipid bilayer membranes were obtained by painting solutions of 1,2-diphytanoyl-*sn*-glycero-3-phosphocholine (Avanti Polar Lipids, Alabaster, AL). The bulk solution in both the *cis*- and the *trans*-compartment contained 200 mM NaCl, 10 mM $MgCl_2$, 50 mM Tris/HCl pH 7.6. The pore conductance was measured for membrane potentials from −150 to +150 mV. Different samples of affinity purified TraB were used.

To prove that the single channel recordings were caused by TraB and not by co-purified contaminating proteins, several control experiments, described in the text (Supplementary Figure S9), were carefully performed.

Bioinformatics

To identify homologues of plasmid-encoded TraB proteins, we searched the non-redundant database at NCBI using PSI-BLAST (Altschul *et al*, 1997). Members of the FtsK/SpoIIIE family were retrieved as the closest homologues based on the presence of a highly similar DNA-translocase domain.

To search for homologues of known structure, we employed HHpred (Soding *et al*, 2005), a remote homology detection method based on the comparison of profile hidden Markov models. Searches with TraB proteins against the protein data bank (PDB) (Berman *et al*, 2000), as available on 6 March 2010, clustered at 70% pairwise sequence identity found the DNA-translocase domains *E. coli* and *P. aeruginosa* FtsK, PDB identifiers 2IUS and 2IUT, respectively (Massey *et al*, 2006), as the closest homologues. Additionally, the C-terminal parts of TraB proteins showed significant sequence similarity to the γ-domain of FtsK, PDB-ID 2J5P, which adopts a wHTH fold (Sivanathan *et al*, 2006).

We extracted the C-terminal wHTH domains of TraB proteins based on HHpred alignments to the γ-domain of FtsK. The multiple alignment of the TraB wHTH domains and FtsK γ-domains in Supplementary Figure S3 was generated with PROMALS 3D (Pei *et al*, 2008) and edited based on alignments obtained from HHpred.

Multiple sequence alignments of the DNA-translocase domain of selected FtsK and TraB proteins for phylogenetic inference were built using PROMALS 3D (Pei *et al*, 2008). Phylogenetic analysis was conducted with PHYLIP-NEIGHBOR using the JTT model (Felsenstein, 1996). The consensus phylogenetic tree is presented with FigTree (http://tree.bio.ed.ac.uk/software/figtree/).

Homology models of the TraB wHTH domains were generated with Modeller (Sali and Blundell, 1993) using the γ-domain of FtsK of *P. aeruginosa* bound to KOPS-DNA as a template (2VE9; Löwe *et al*, 2008). The crystal structure of the hexameric DNA-translocase domain of FtsK of *P. aeruginosa*, 2IUU (Massey *et al*, 2006), served as a template for modelling the corresponding domain of $TraB_{pSVH1}$ in an oligomeric state. Symmetry restraints applied to chains B to F ensured six-fold symmetry. Molecular structures shown in Figures 2 and 6 were rendered using PyMol (http://pymol.org).

Supplementary data

Supplementary data are available at *The EMBO Journal* Online (http://www.embojournal.org).

Acknowledgements

We thank T Arnold for advice on lipid bilayer measurements, T Weber for performing PatScan analyses, Stanislaw Dunin-Horkawicz for bioinformatic support and S Ludtke for providing EMAN Suite and his support. We are grateful to V Braun and J Schultz for helpful comments on the manuscript and to the DFG (SFB766) for financial support.

Author contributions: JV and GM designed the experiments and wrote the paper with contributions from DL, MA and WW. JV performed the experiments with contributions of CF, JG and MA. EM analysis was performed by MF and YS. MA performed bioinformatic analyses and homology modelling. DL supervised lipid bilayer measurements. All authors discussed the results and commented on the article.

Conflict of interest

The authors declare that they have no conflict of interest.

References

Altschul SF, Madden TL, Schäffer AA, Zhang J, Zhang Z, Miller W, Lipman DJ (1997) Gapped BLAST and PSI-BLAST: a new generation of protein database search programs. *Nucleic Acids Res* **25:** 3389–3402

Alvarez-Martinez CE, Christie PJ (2009) Biological diversity of prokaryotic type IV secretion systems. *Microbiol Mol Biol Rev* **73:** 775–808

Berman HM, Westbrook J, Feng Z, Gilliland G, Bhat TN, Weissig H, Shindyalov IN, Bourne PE (2000) The protein data bank. *Nucleic Acids Res* **28:** 235–242

Bigot S, Saleh OA, Lesterlin C, Pages C, El Karoui M, Dennis C, Grigoriev M, Allemand JF, Barre FX, Cornet F (2005) KOPS: DNA motifs that control *E. coli* chromosome segregation by orienting the FtsK translocase. *EMBO J* **24:** 3770–3780

Brennan RG (1993) The winged-helix DNA-binding motif: another helix-turn-helix take off. *Cell* **74:** 773–776

Burton BM, Marquis KA, Sullivan NL, Rapoport TA, Rudner DZ (2007) The ATPase SpoIIIE transports DNA across fused septal membranes during sporulation in *Bacillus subtilis*. *Cell* **131:** 1301–1312

Chandran V, Fronzes R, Duquerroy S, Cronin N, Navaza J, Waksman G (2009) Structure of the outer membrane complex of a type IV secretion system. *Nature* **462:** 1011–1015

Christie PJ, Atmakuri K, Krishnamoorthy V, Jakubowski S, Cascales E (2005) Biogenesis, architecture, and function of bacterial type IV secretion systems. *Annu Rev Microbiol* **59:** 451–485

Davies J (1994) Inactivation of antibiotics and the dissemination of resistance genes. *Science* **264:** 375–382

de la Cruz F, Frost LS, Meyer RJ, Zechner EL (2010) Conjugative DNA metabolism in Gram-negative bacteria. *FEMS Microbiol Rev* **34:** 18–40

D'Costa VM, McGrann KM, Hughes DW, Wright GD (2006) Sampling the antibiotic resistome. *Science* **311:** 374–377

Dsouza M, Larsen N, Overbeek R (1997) Searching for patterns in genomic data. *Trends Genet* **13:** 497–498

Dubarry N, Barre FX (2009) Fully efficient chromosome dimer resolution in *Escherichia coli* cells lacking the integral membrane domain of FtsK. *EMBO J* **29:** 597–605

Felsenstein J (1996) Inferring phylogenies from protein sequences by parsimony, distance, and likelihood methods. *Methods Enzymol* **266:** 418–427

Franco B, Gonzalez-Ceron G, Servin-Gonzalez L (2003) Direct repeat sequences are essential for function of the cis-acting locus of transfer (*clt*) of *Streptomyces phaeochromogenes* plasmid pJV1. *Plasmid* **50:** 242–247

Garcillán-Barcia MP, Jurado P, González-Pérez B, Moncalián G, Fernández LA, de la Cruz F (2007) Conjugative transfer can be inhibited by blocking relaxase activity within recipient cells with intrabodies. *Mol Microbiol* **63:** 404–416

Gomis-Rüth FX, Moncalián G, Pérez-Luque R, González A, Cabezón E, de la Cruz F, Coll M (2001) The bacterial conjugation protein TrwB resembles ring helicases and F1-ATPase. *Nature* **409:** 637–641

Grohmann E, Muth G, Espinosa M (2003) Conjugative plasmid transfer in gram-positive bacteria. *Microbiol Mol Biol Rev* **67:** 277–301

Gunton JE, Gilmour MW, Baptista KP, Lawley TD, Taylor DE (2007) Interaction between the co-inherited TraG coupling protein and the TraJ membrane-associated protein of the H-plasmid conjugative DNA transfer system resembles chromosomal DNA translocases. *Microbiology* **153:** 428–441

Higuchi R, Krummel B, Saiki RK (1988) A general method of *in vitro* preparation and specific mutagenesis of DNA fragments: study of protein and DNA interactions. *Nucleic Acids Res* **16:** 7351–7367

Hopwood DA, Kieser T (1993) Conjugative plasmids of *Streptomyces*. In *Bacterial Conjugation*, Clewell DB (ed) pp 293–311. New York: Plenum Press

Iyer LM, Makarova KS, Koonin EV, Aravind L (2004) Comparative genomics of the FtsK-HerA superfamily of pumping ATPases: implications for the origins of chromosome segregation, cell division and viral capsid packaging. *Nucleic Acids Res* **32:** 5260–5279

Karimova G, Pidoux J, Ullmann A, Ladant D (1998) A bacterial two-hybrid system based on a reconstituted signal transduction pathway. *Proc Natl Acad Sci USA* **95:** 5752–5756

Kieser T, Hopwood DA, Wright HM, Thompson CJ (1982) pIJ101, a multi-copy broad host-range *Streptomyces* plasmid: functional analysis and development of DNA cloning vectors. *Mol Gen Genet* **185:** 223–238

Kieser T, Bibb MJ, Buttner MJ, Chater KF, Hopwood DA (2000) *Practical Streptomyces Genetics*. Norwich: The John Innes Foundation

Lederberg J, Tatum EL (1946) Gene recombination in *Escherichia coli*. *Nature* **158:** 558

Löwe J, Ellonen A, Allen MD, Atkinson C, Sherratt DJ, Grainge I (2008) Molecular mechanism of sequence-directed DNA loading and translocation by FtsK. *Mol Cell* **31:** 498–509

Ludtke SJ, Baldwin PR, Chiu W (1999) EMAN: semiautomated software for high-resolution single-particle reconstructions. *J Struct Biol* **128:** 82–97

Massey TH, Mercogliano CP, Yates J, Sherratt DJ, Lowe J (2006) Double-stranded DNA translocation: structure and mechanism of hexameric FtsK. *Mol Cell* **23:** 457–469

Miller JB, Koshland Jr DE (1977) Sensory electrophysiology of bacteria: relationship of the membrane potential to motility and chemotaxis in *Bacillus subtilis*. *Proc Natl Acad Sci USA* **74:** 4752–4756

Pettis GS, Cohen SN (1994) Transfer of the pIJ101 plasmid in *Streptomyces lividans* requires a *cis*-acting function dispensable for chromosomal gene transfer. *Mol Microbiol* **13:** 955–964

Pei J, Kim BH, Grishin NV (2008) PROMALS3D: a tool for multiple protein sequence and structure alignments. *Nucleic Acids Res* **36:** 2295–2300

Possoz C, Ribard C, Gagnat J, Pernodet JL, Guerineau M (2001) The integrative element pSAM2 from *Streptomyces*: kinetics and mode of conjugal transfer. *Mol Microbiol* **42:** 159–166

Ptacin JL, Nollmann M, Becker EC, Cozzarelli NR, Pogliano K, Bustamante C (2008) Sequence-directed DNA export guides chromosome translocation during sporulation in *Bacillus subtilis*. *Nat Struct Mol Biol* **15:** 485–493

Reuther J, Wohlleben W, Muth G (2006a) Modular architecture of the conjugative plasmid pSVH1 from *Streptomyces venezuelae*. *Plasmid* **55:** 201–209

Reuther J, Gekeler C, Tiffert Y, Wohlleben W, Muth G (2006b) Unique conjugation mechanism in mycelial streptomycetes: a DNA-binding ATPase translocates unprocessed plasmid DNA at the hyphal tip. *Mol Microbiol* **61:** 436–446

Sali A, Blundell TL (1993) Comparative protein modelling by satisfaction of spatial restraints. *J Mol Biol* **234:** 779–815

Sambrook J, Russel DW (2001) *Molecular Cloning—A Laboratory Manual*. New York: Cold Spring Harbor Laboratory Press

Schröder G, Lanka E (2003) TraG-like proteins of type IV secretion systems: functional dissection of the multiple activities of TraG (RP4) and TrwB (R388). *J Bacteriol* **185:** 4371–4381

Servín-González L (1996) Identification and properties of a novel *clt* locus in the *Streptomyces phaeochromogenes* plasmid pJV1. *J Bacteriol* **178:** 4323–4326

Sivanathan V, Allen MD, de Bekker C, Baker R, Arciszewska LK, Freund SM, Bycroft M, Löwe J, Sherratt DJ (2006) The FtsK gamma domain directs oriented DNA translocation by interacting with KOPS. *Nat Struct Mol Biol* **13:** 965–972

Soding J, Biegert A, Lupas AN (2005) The HHpred interactive server for protein homology detection and structure prediction. *Nucleic Acids Res* **33:** W244–W248

Tang G, Peng L, Baldwin PR, Mann DS, Jiang W, Rees I, Ludtke SJ (2007) EMAN2: an extensible image processing suite for electron microscopy. *J Struct Biol* **157:** 38–46

Thomas CM, Nielsen KM (2005) Mechanisms of, and barriers to, horizontal gene transfer between bacteria. *Nat Rev Microbiol* **3:** 711–721

Willets N, Wilkins B (1984) Processing of plasmid DNA during bacterial conjugation. *Microbiol Rev* **48:** 24–41

Ursinus A, van den Ent F, Brechtel S, de Pedro M, Höltje JV, Löwe J, Vollmer W (2004) Murein (peptidoglycan) binding property of the essential cell division protein FtsN from Escherichia coli. *J Bacteriol* **186:** 6728–6737

Yu XC, Tran AH, Sun Q, Margolin W (1998) Localization of cell division protein FtsK to the Escherichia coli septum and identification of a potential N-terminal targeting domain. *J Bacteriol* **180:** 1296–1304

Zechner EL, de la Cruz F, Eisenbrandt R, Grahn AM, Koraimann G, Lanka E, Muth G, Pansegrau W, Thomas CM, Wilks M, Zatyka M (2000) Conjugative-DNA transfer processes. In *The Horizontal Gene Pool*, Thomas CM (ed) pp 87–175. Amsterdam: Harwood Academic Publishers

